

Preliminary assessment of wave energy hazards in a shallow underwater cultural heritage site

George Alexandrakis¹, Stelios Petrakis², Nikolaos Kampanis¹

¹ *Foundation for Research and Technology - Hellas, Institute of Applied and Computational Mathematics (FORTH-IACM), N. Plastira 100, 70013 Heraklion, Greece,*
alexandrakis@iacm.forth.gr, kampanis@iacm.forth.gr

² *Institute of Oceanography, Hellenic Centre for Marine Research (HCMR), 46.7 km Athens-Sounion, s.petrakis@hcmr.gr*

Abstract – Coastal areas are characterized by high energetic conditions associated with the wave transformation processes and by numerous underwater cultural heritage (UCH) sites whose preservation is crucial given their cultural and economic value. Wave energy is considered a significant hazard driver for the conservation of UCH sites in wave-exposed coasts and may cause the scattering and scouring of archaeological objects, which results in the loss and degradation of the sites. In this paper, the wave energy-induced threats of a coastal site that was revealed due to coastal erosion in the mid-1970s and now is completely submerged in shallow waters, is examined. The results showed that wave energy is a significant threat due to the scouring and weathering phenomena that can detach materials from the structure.

I. INTRODUCTION

Many underwater cultural heritage (UCH) sites are in coastal areas because of the intense use of those areas for human settlement. Coastal areas are also prone to coastal hazards such as stormy weather conditions and wave energy. Furthermore, shallow coastal waters are highly energetic environments where oceanographic factors such as waves, currents, and sediment transport form a dynamic environmental setting. Changes in the coastal environmental conditions can generate successive burial and exposure of UCH sites [1], affecting the stability and degradation of UCH sites [2,3]. Additionally, coastal erosion and sediment transport can remove layers of sediments that act as protective covers for certain archaeological objects [2]. Therefore, the degradation of UCH sites [3,4] may be aggravated in shallow water areas. At the UCH sites located in coastal waters, the degradation rates may experience episodic oscillations associated with changes in the environmental conditions in the area [5].

Wave energy is considered a significant hazard driver for the conservation of UCH sites in wave-exposed coasts and may cause the scattering and scouring of archaeological objects which result in the loss and degradation of such

sites. Wave-induced flow and turbulence may lead to scouring around UCH sites [6,7]. Wave-induced scour may vary depending on the structure's size and wave conditions [7,8], since it largely controls the integrity of the UCH sites.

Therefore, considering that many UCH sites are in coastal areas it is critical to assess the hazardous conditions linked to wave energy to identify areas under threat. This need is increased under the context of climate change and the changes in wave regime [9]. The present work aims to provide a preliminary assessment of the threat of a semi-submerged archeological site that was revealed due to coastal erosion.

II. STUDY AREA

The study area is a complex of sunken historical buildings at Stomio in Ierapetra, Crete in Greece (Fig. 1). The site was first mentioned by Dermitzakis [10]. In 1985, Mourtzas [11], thoroughly described the site and published their building plans.



Fig. 1. Study Area

The building complex of Stomio has for the most part been destroyed due to wave energy and human interventions to tackle coastal erosion [12]. During the survey of Mourtzas, in 1985, it was found that the building complex consisted of five distinct sections. The building

complex had traces inland until 2012, and since then the inland traces were lost or destroyed. Based on the architectural and structural features of the building complex it was dated to the period of its Roman occupation of Crete, between 69 BC and 369 AD, while similar architectures and structural features are seen in the Roman baths that have been located at other nearby sites.

III. METHODS

A. Environmental factors

Geomorphological and sedimentological mapping of the area was conducted with the use of satellite images, drone imagery, and field surveys. For the geomorphological mapping, topographic diagrams from the Hellenic Army Geographical Service and Sentinel satellite images were used. The geomorphological surveys included elevation and slope measurements taken with an RTK GPS. Additionally, depth soundings were acquired using a single beam echo-sounder reaching 20 m depth within the water. Such data were synthesized to create current bathymetry and beach elevations. Furthermore, surficial sediment samples were collected along the beach and analyzed. The conducted seafloor survey includes sediment sampling, Side Scan Sonar image survey, and ROV photographic documentation.

Aerial photographs and satellite images were used to study the stability of the coastline and to measure its displacement over time. Based on these data, the coastlines were digitized with the utmost accuracy through ArcGIS 10.1 software, through which conclusions were drawn for the shoreline displacement over time. This was followed by processing with Digital Shoreline Analysis System DSAS v.5 to quantify the changes. Three different types of remote sensing data—historical analog panchromatic aerial photographs, orthophotos, and natural-color satellite images—were used for the identification of the beach area alterations during the last 77 years. The acquisition of the aerial photographs took place in 1945, 1968, and 1998 from Hellenic Military Geographical Service (HMGS); the orthophotos were acquired in 2005 and 2010 from Ktimatologio S.A; and the satellite images during 2009, 2012, 2013, 2016, 2017, 2019 and 2022.

For the calculation of the wave climate of the area, the significant wave height H_s , the peak energy period T_s , and the mean period T_z were estimated by the JONSWAP model. Wave estimations were made for wind waves from 5 directions in origin (N, NW, NE, E, and W). The spectral significant wave height and spectral period calculated are the maximum values that can be derived for the maximum wind speed. The minimum required duration for the winds affecting the area is within the range observed in the wider area and therefore the assumption is that the maximum wave growth is only limited by wind blowing. To study the distribution of wave energy along the coast in the area, wave refraction diagrams were constructed using Delft-

3D. For each wave direction affecting the coastal zone, refraction diagrams for waves with higher wavelengths were constructed, as well as the usual peak values for the area calculated on a weighted average basis for the incidence.

B. Hazards Assessment

The materials detachment of a UCH artefact occurs when drag forces induced by waves on the seabed are sufficient to transport objects located in the UCH site. Furthermore, wave forces and wave loads can damage and transport part of the damaged structure away from the site, producing the disintegration and decay of the archaeological structure [13]. The potential damage of scattering and loss of archaeological artifacts induced by waves was evaluated using Eq. 1 as proposed by Soulsby [14] for the threshold motion of large-diameter particles, considering the sole action of wind waves,

$$D_{cr} = \sqrt{\left(\frac{97.9U_b^{3.08}}{T_p \left[g \left(\frac{p_s}{p} \right) - 1 \right]^{2.08}} \right)} \quad (1)$$

where U_b is the undisturbed near-bed orbital velocity, T_p is the peak wave period, g is the gravitational constant, p_s is the density of the grain sediment, and p is the seawater density.

The scattering and loss of archaeological objects at UCH sites depend on the material, size, and shape of the archaeological objects.

The potential scouring was estimated using the equilibrium scour depth. Calculating the equilibrium scour depth was based on Eq. 2 for maximum scour depth and Eq. 3 [15] for the maximum scour length for wave-induced scour on pipelines. A constant archaeological object/structure of a cylindrical shape of 1 m in diameter was assumed.

$$L_{Smax} = 0.35 \cdot D \cdot KC^{0.65} \quad (2)$$

where KC is the Keulegan–Carpenter dimensionless number

$$KC = \frac{U_b \cdot T_p}{D} \quad (3)$$

U_b is the maximum undisturbed near-bed orbital velocity, T_p is the peak wave period, and D is the structure diameter.

In the case of breaking or near-breaking wave conditions, the equilibrium scour depth was calculated according to expressions Eq. 4 and Eq. 5 proposed by Young and Testik [16] for vertical and semicircular breakwaters applied for conditions $0.6 < KCH \leq 9.0$ and $0.4 < f_b \leq 1.7$, where KCH is the Keulegan–Carpenter number expressed as a function of the significant wave height (H_s) $KCH = H_s \cdot p / D$, and f_b is the ratio of the water depth over structure height, i.e. $f_b = (h - D) / H_s$, where h is the water depth, and D is the structure diameter.

$$S_{max} = 0.125 \cdot D \cdot KC_{H_s} \sqrt{\psi} \quad (5)$$

$$L_{smax} = \begin{cases} 0.5 \cdot D \cdot KC_{Hs}, & KC > \pi \text{ detached scour} \\ D \cdot KC_{Hs}, & KC \leq \pi \text{ attached scour} \end{cases} \quad (6)$$

where Ψ the mobility number

$$\Psi = \frac{\left(\frac{\pi \cdot H_s}{T \cdot \sinh(kh)}\right)^2}{g \cdot d} \quad (7)$$

where g is the reduced gravitational acceleration, d is the median diameter of the sediment, k is the wave number, h is water depth, and T is the wave period. Together, equations 5 and 6 allow calculating the maximum scour depth and the length of the scour hole.

Weathering hazard refers to the erosive wear caused by solid particle erosion, the process that occurs on archaeological structures artifacts in the seabed exposed to the impact of suspended sediment particles transported by waves. The optimal approach to evaluate this hazard includes estimating the volume of material eroded by a single grain impact (U_i) according to the impact wear equation proposed by Bitter [17]. However, this approach requires specific measurements and the details of the threshold energy required for impact as well as the kinetic energy necessary to erode a unit of volume of material, depending on the status of the different archaeological materials. Therefore, the erosive wear potential is used as an erosive wear hazard indicator, and it is calculated using kinetic energy.

$$KE = 0.5 \cdot (M_{sp} \cdot U_i^2) \quad (8)$$

where U_i is the grain velocity and M_{sp} is the mass of the particle) of the impacting grain considering the direction that maximizes the erosion ($\alpha=90^\circ$) multiplied by the impact rate [18].

IV. RESULTS

The End Point Rate (EPR) shows the rate at which the coastline moves during the period of study for the area (1945-2023). The unit of measurement is meters/time. Note that EPR does not account for intermediate shoreline shifts between the oldest and youngest. As shown in Fig. 2, the average rate of displacement for the entire western part of the study area is -0.4 meters per year, while considering only the trenches in which the retreat occurs, the average rate of retreat reaches 0.45 meters per year. The maximum observed regression rate is 0.8 meters per year around Stomio with a regression of the trend of 0.7-0.8 m/hr.

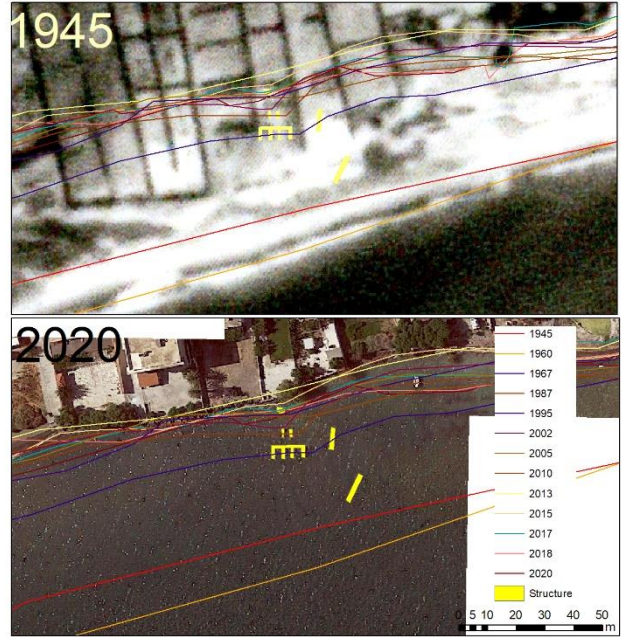


Fig. 2 Coastline retreat in the 1945-2020 period

To study the distribution of wave energy along the coast in the area, wave refraction diagrams were constructed using numerical models. For each wave direction affecting the coastal zone, refraction diagrams for waves with higher wavelengths were constructed, as well as the usual peak values for the area were calculated on a weighted average basis for the incidence. The wave characteristics used in numerical modeling are presented in table 1.

Table 1. Wave characteristics used in numerical modeling

Direction	Hs (m)	Ts (sec)
S	1,26	5,91
S	5,06	10,05
SE	1,15	5,66
SE	4,54	9,69
SW	1,37	6,16
SW	6,21	11,49
E	1,22	5,82
E	5,47	10,67
W	1,71	6,89
W	5,77	10,96

South-direction waves approach the coastline in the works in a vertical direction and with their peaks parallel to it. The average wave height ranges between 1.5 m and 2.5 m for waves induced by winds of medium intensity. The wave height increases for maximum south waves and reaches 3.5 m to 4.5 m. As far as the coastal current of

wave origin is concerned, and for all wave intensities, in the fracture zone it shows direction to the east but mainly vertically. In Stomio, the current moves in the opposite direction, that is East and creates the erosion phenomena in the area. The intensity of the coastal current increases with the intensity of the waves. Sediment transport follows a similar movement to that of wave currents, with its values increasing for waves with a significant wave height greater than 4m.

The waves of the southeast direction approach the coastline in the area with a small angle and with their peaks almost parallel to it, due to refraction. The average wave height ranges between 1.5 m and 2 m for waves coming from winds of medium intensity. The wave height increases for maximum southbound ripples and reaches 3.5 m to 4.5 m. As far as the coastal current, and for all wave intensities, in the fracture zone it shows a direction to the west. The intensity of the coastal current increases with the intensity of the waves. Regarding sediment transport, there is a similar movement to that of wave currents, with its values increasing for waves with a significant wave height greater than 4m.

The waves of the southwest direction approach the coastline in the works in a vertical direction and with their peaks parallel to it. The average wave height ranges between 1.5 m and 2.5 m for waves coming from winds of medium intensity. The wave height increases for maximum waves of SW direction and reaches 3.5 m to 4.5 m. As far as the coastal current of wave origin is concerned, and for all wave intensities, the area of the fracture zone shows an eastbound direction. Regarding coastal sediment transport, there is a similar movement to that of wave currents, with its values increasing for waves with a significant wave height greater than 4m.

The erosive wear hazard ranges from -16 to -12. Most of the area is characterized by -13.5. The higher erosion potential (< -12.5) was observed on the north side of the buildings since the kinetic energy of the waves was found higher in the onshore-offshore direction. These areas combine higher wave bed shear stress and orbital velocity with finer sediment that can be easily resuspended. An example of the bottom layer wave forcing for south-direction waves is presented in Fig. 3.

A potential scour volume of 0.32 m^3 is observed in most of the area, while values $>0.5 \text{ m}^3$ can be observed in the south part of the walls and on their east side. The scouring on those sides increases the danger of collapsing. An example of a scouring effect on the side is presented in Fig. 4.

Regarding the detachment hazard, it was found that waves can detach rock objects that have diameters greater than 0.5 m. This indicates that parts of the walls of the structures could have been removed from the structure after its exposure to the waves sometime in the late 1970s when the structure had started to be affected by the waves due to coastal erosion.

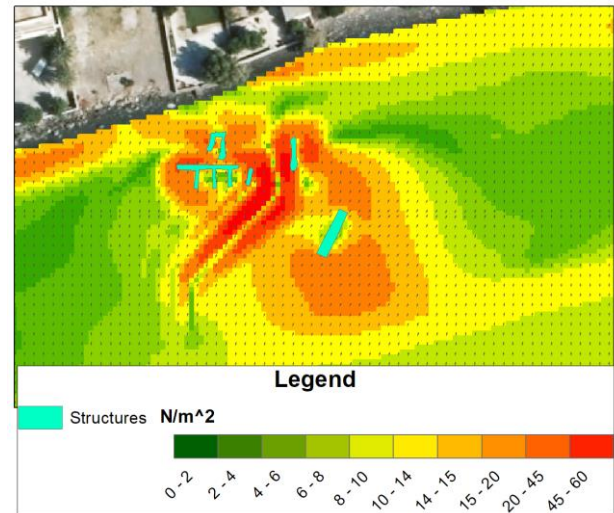


Fig. 3. Bottom layer wave forcing for south direction waves.



Fig. 4. Scouring effect in a wall of the structure

V. CONCLUSIONS

This work aims to estimate the problems caused by the wave impact in the Roman building complex in Stomio, Crete. The results have shown that the main impacts are from the S, SE, E, and SW origin waves, which influence the area and impact mechanical stresses on the site, and have significant erosion events. The problem of the degradation of the Roman building complex was found that started with the uncontrolled exposure of the building due to coastal erosion processes. After the exposure of the site, its submersion began due to the retreating coastline. This added more pressure to the site since the influence of the waves increased the threats due to scouring effects, sediment transport but also to the detachment of materials for the remaining walls. Additionally, parts of the original structure have been buried with wave transport sediments but also from coastal protection works, that were used to protect the modern properties in the coastal front.

As a part of maritime cultural heritage, UCH constitutes

a non-renewable cultural resource that must be preserved. Wave-induced hazards among others, present a significant threat for the preservation of UCH in shallow water. Identifying the wave induced risks of UCH sites is the first step in their protection and preservation.

REFERENCES

- [1] Fernández-Montblanc et al., 2018 Fernández-Montblanc, T., Izquierdo, A., Quinn, R., and Bethencourt, M. (2018). Waves and wrecks: A computational fluid dynamic study in an underwater archaeological site. *Ocean Eng.* 163, 232–250. doi: 10.1016/j.oceaneng.2018.05.062
- [2] Bethencourt et al., 2018; 3 Bethencourt, M., Fernández-Montblanc, T., Izquierdo, A., González-Duarte, M. M., and Muñoz-Mas, C. (2018). Study of the influence of physical, chemical and biological conditions that influence the deterioration and protection of underwater cultural heritage. *Sci. Total Environ.*, 613–614, 98–114. doi: 10.1016/j.scitotenv.2017.09.007
- [3] Gregory, 2020 Gregory, D. (2020). Characterizing the preservation potential of buried marine archaeological sites. *Herit* 3, 838–857. doi: 10.3390/HERITAGE3030046
- [4] Pournou, 2018 Pournou, A. (2018). Assessing the long-term efficacy of geotextiles in preserving archaeological wooden shipwrecks in the marine environment. *J. Marit. Archaeol.* 13, 1–14. doi: 10.1007/S11457-017-9176-9
- [5] Ward et al., 1999 Ward, I. A. K., Larcombe, P., and Veth, P. (1999). A new process-based model for wreck site formation. *J. Archaeol. Sci.* 26, 561–570. doi: 10.1006/JASC.1998.0331
- [6] Fernández-Montblanc et al., 2016 Fernández-Montblanc, T., Quinn, R., Izquierdo, A., and Bethencourt, M. (2016) Evolution of a shallow water wave-dominated shipwreck site: Fougueux, (1805), Gulf of Cadiz. *Geoarchaeology* 31, 487–505. doi: 10.1002/gea.21565
- [7] Quinn, 2006 Quinn, R. (2006). The role of scour in shipwreck site formation processes and the preservation of wreck-associated scour signatures in the sedimentary record - evidence from seabed and sub-surface data. *J. Archaeol. Sci.* 33, 1419–1432. doi: 10.1016/J.JAS.2006.01.011
- [8] McNinch, J. E., Wells, J. T., and Trembanis, A. C. (2006). Predicting the fate of artefacts in energetic, shallow marine environments: an approach to site management. *Int. J. Naut. Archaeol.* 35, 290–309. doi: 10.1111/j.1095-9270.2006.00105.x
- [9] Mentaschi, L., Vousdoukas, M. I., Voukouvalas, E., Dosio, A., and Feyen, L. (2017). Global changes of extreme coastal wave energy fluxes triggered by intensified teleconnection patterns. *Geophys. Res. Lett.* 44, 2416–2426. doi: 10.1002/2016GL072488
- [10] Dermitzakis 10 (1973 Dermitzakis 1973: M. Dermitzakis, Recent Tectonic Movements and Old Strandlines Along the Coasts of Crete. *Bulletin of the Geological Society* 10, 48 - 64.
- [11] Mourtzas 1988: N. Mourtzas, Archaeological Constructions as Indicators of the Sea-level During the Last 2000 Years in the Area of Ierapetra (SE Crete, Greece), *ιπ*: P. Marino~ G. Koukis (edsλ The Engineering Geology of Ancient Works/ Monuments and Historical Sites/ Balkema/ v. ι~ 1557 - 1564.
- [12] Kolaiti, Eleni & Mourtzas, Nikos. (2019). Archaeological indicators of the relative sea level change along the coast of Ierapetra since Roman times.. Conference: 2nd International Conference: "Ancient, Byzantine and Modern Monuments of Ierapetra", 16-17 June 2017At: Ierapetra, Crete, GreeceVolume: p. 86-108
- [13] Ward et al., 1999 Ward, I. A. K., Larcombe, P., and Veth, P. (1999). A new process-based model for wreck site formation. *J. Archaeol. Sci.* 26, 561–570. doi: 10.1006/JASC.1998.0331
- [14] Soulsby (14 1997 Soulsby, R. L., and Clarke, S. (2005). Bed shear-stresses under combined waves and currents on smooth and rough beds produced within defra project FD1905 Technical Report. Wallingford: HR Wallingford.
- [15] Sumer and Fredsøe, 1990 Sumer, B. M., and Fredsøe, J. (2002). The mechanics of scour in the marine environment. *World Sci Sinagpore.* doi: 10.1142/4942
- [16] Young and Testik (16 2009 Young, D. M., and Testik, F. Y. (2009). Onshore scour characteristics around submerged vertical and semicircular breakwaters. *Coast. Eng.* 56, 868–875. doi: 10.1016/J.COASTALENG.2009.04.003
- [17] Bitter (17 1963 Bitter, J. G. A. (1963). A study of erosion phenomena part I. *Wear* 6, 5–21. doi: 10.1016/0043-1648(63)90003-6
- [18] Thompson et al., 2011 Thompson, C. E. L., Ball, S., Thompson, T. J. U., and Gowland, R. (2011). The abrasion of modern and archaeological bones by mobile sediments: the importance of transport modes. *J. Archaeol. Sci.* 38, 784–793. doi: 10.1016/J.JAS.2010.11.001